Journal of Thrombosis and Haemostasis, **4**: 443–452

ORIGINAL ARTICLE

ERK2 activation in arteriolar and venular murine thrombosis: platelet receptor GPIb vs. $P2X_1$

C. OURY,*[1] K. DAENENS,*[1] H. HU,* E. TOTH-ZSAMBOKI,* M. BRYCKAERT† and M. F. HOYLAERTS*
*Center for Molecular and Vascular Biology, University of Leuven, Leuven, Belgium; and †Hopital Lariboisière, U689 INSERM, IFR139, Paris, France

To cite this article: Oury C, Daenens K, Hu H, Toth-Zsamboki E, Bryckaert M, Hoylaerts MF. ERK2 activation in arteriolar and venular murine thrombosis: platelet receptor GPIb vs. $P2X_1$. *J Thromb Haemost* 2006; **4**: 443–52.

Summary. The functional significance of extracellular signal-regulated kinase 2 (ERK2) activation was investigated during shear induced human platelet aggregation (SIPA) *in vitro* and during shear controlled thrombosis *in vivo* in intestinal arterioles and venules of wild type (WT) and transgenic (TG) mice with platelet-specific overexpression of human $P2X_1$ (TG). In SIPA, ERK2 was rapidly phosphorylated during GPIb stimulation, its activation contributing to SIPA for 50%, independently of $P2X_1$ regulation. Thrombotic occlusion of injured arterioles occurred considerably faster in TG (4.3 ± 2.3 min) than in WT (38 ± 8 min) arterioles, but occlusion times in TG (19 ± 12) and WT (48 ± 4.5 min) venules differed less. Both the αβ-meATP triggered desensitization of platelet $P2X_1$, as well as $P2X_1$ antagonism by NF279 or NF449 prolonged mean occlusion to about 75 min in WT and 65 min in TG arterioles, but venular occlusion times were less affected. Preventing ERK2 activation by U0126 prolonged occlusion times in TG (41 ± 10 min) and WT (51 ± 17) arterioles more than in TG (46 ± 5 min) and WT (56 ± 6 min) venules, uncovering a role for ERK2 in shear controlled thrombosis. Antagonism of GPIb by a recombinant murine von Willebrand factor (VWF)-A1 fragment prolonged occlusion times to comparable values, ranging from 55 to 58 min, both in TG and WT arterioles and venules. Further inhibition strategies, combining VWF-A1, U0126 and NF449 in WT and TG mice and resulting in occlusion in various time windows, identified that inhibition by VWF-A1 largely abrogated the ERK2 contribution to thrombosis. In conclusion, $P2X_1$ and ERK2 both participate in shear stress controlled thrombosis, but ERK2 activation is initiated predominantly via GPIb–VWF interactions.

Keywords: degranulation, nucleotides, platelet, shear stress, signaling, thrombosis.

Correspondence: Marc Hoylaerts, Center for Molecular and Vascular Biology, University of Leuven, Campus Gasthuisberg, Herestraat 49, B-3000 Leuven, Belgium.
Tel.: +32 16 346 145; fax: +32 16 345 990; e-mail: marc.hoylaerts@med.kuleuven.ac.be

Present addresses: C. Oury, Center of Biomedical Integrative Genoproteomics, University of Liège, Belgium.
E. Toth-Zsamboki, Cardiovascular Research Group of the Hungarian Academy of Sciences and Semmelweis University, Budapest, Hungary.

[1]Contributed equally to this work.

Received 1 September 2005, accepted 21 October 2005

Introduction

Upon blood vessel injury, circulating platelets tether to the vessel wall, form a plug and arrest bleeding [1]. Platelets interact with subendothelial von Willebrand factor (VWF) via platelet glycoprotein Ibα (GPIbα) and with collagen fibers via platelet GPVI and $\alpha_2\beta_1$ [2–5]. Adhering platelets undergo morphological changes, synthetize thromboxane A_2 (TxA_2), secrete ATP and ADP from dense granules and several proteins from α-granules [6], each of them interacting with specific platelet receptors and leading to further recruitment and activation of platelets [7–9], processes exacerbated during atherothrombotic disease [10].

Platelets express three known P2 receptors for adenine nucleotides: the GTP binding protein-coupled $P2Y_1$ and $P2Y_{12}$ receptors, activated by ADP, and the ATP-gated $P2X_1$ ion channel [11,12]. Gi-coupled $P2Y_{12}$ plays a central role in platelet activation and is a pharmacological target for $P2Y_{12}$ antagonists [13] and thienopyridines [14]. Studies in $P2Y_{12}$-deficient mice revealed that this receptor is involved in thrombus growth and stability and that its gene deficiency markedly impacts on thrombosis [15]. Gq-coupled $P2Y_1$ is also involved in thrombus growth and its antagonism in mice has equally proven to be antithrombotic [16]. Overexpression of $P2X_1$ ion channels in the megakaryocytic cell lineage of transgenic (TG) mice generates a prothrombotic phenotype [17]. That study and analysis of platelet function in $P2X_1$-null mice [18] indicated that $P2X_1$ contributes to thrombus formation, particularly in conditions in which shear forces are high. Notably, in $P2X_1$-null mice, the size of mural thrombi formed after laser-induced arterial wall injury was decreased and the time for complete thrombus removal was shortened [18].

Via the influx of Ca^{2+}, platelet $P2X_1$ mediates activation of the extracellular signal-regulated kinase 2 (ERK2), an event participating in platelet aggregation induced by low concentrations of collagen [19,20]. Accordingly, inhibition of ERK2 activation by the MAPK kinase inhibitor U0126 could considerably reduce mortality in a model of collagen-induced pulmonary embolism, in $P2X_1$ overexpressing TG and in wild type (WT) mice [17]. More recently, we reported a role for $P2X_1$ in shear stress induced platelet activation [21], but also found that the adhesion of platelets to collagen, following perfusion under shear stress conditions involved ERK2 phosphorylation, a process dependent on platelet-VWF interactions [22]. In addition, it has been shown that in platelets, ERK2 is also activated by thrombin [23,24], a process recently having been linked to ADP secretion and subsequent $P2Y_{12}$ receptor signaling [25].

In view of the role of the $P2X_1$-ERK2 axis in *shear stress-independent* platelet activation by collagen, in the present study, we therefore set out to investigate the role of *shear stress-dependent* ERK2 activation in platelets *in vitro* and *in vivo* in a mouse model of arteriolar and venular thrombosis in WT mice, and in mice specifically overexpressing human $P2X_1$ in platelets [17]. We confirmed that $P2X_1$ functions in shear stress controlled thrombosis, to a larger degree in arteriolar than venular thrombosis. Moreover, we identified a role for ERK2 activation in arteriolar and venular thrombosis in both WT and TG mice, its contributions to shear stress controlled thrombosis, however, relying largely on GPIb-VWF initiated signaling, rather than on $P2X_1$-ATP signaling.

Materials and methods

Materials

The $P2X_1$ agonist α,β-methylene adenosine 5′- triphosphate (α,β-meATP), the $P2X_1/P2X_3$ agonist L-β,γ-methylene adenosine 5′-triphosphate (L-β,γ-meATP) and the ectonucleotidase apyrase (grade I) were purchased from Sigma (St Louis, MO, USA). Clopidogrel (Plavix, Sanofi, Toulouse, France) was acquired through the local hospital pharmacy. The $P2X_1$ antagonists NF279 [26] and NF449 [27] were purchased from Tocris (Tocris Cookson, Bristol, UK). The MEK1/2 inhibitor U0126 was purchased from BioMol Research Laboratories (Plymouth Meeting, MA, USA). α,β-meATP and L-β,γ-meATP were purified by HPLC on an Adsorbosphere HS C18, 7 μm, 250x4.6 mm, column (Alltech) as described [28]. Equine tendon collagen type I fibrils (collagen reagent Horm) were from Nycomed (Munich, Germany) and human serum albumin from the local hospital pharmacy.

Murine platelet-rich plasma, washed platelets and platelet aggregation analyses

Eight- to 12-week-old mice were bled under sodium pentobarbital anesthesia (25–35 mg kg^{-1}) from the retroorbital plexus. Mouse blood was collected in a 1/10 volume saline solution containing 200 μg mL^{-1} hirudin and 20 μM PPACK. Platelet-rich-plasma (PRP) was obtained by centrifugation at 800 ***g*** for 30 s followed by 5 min at 150 ***g***. PRPs from three animals were pooled, and the platelet counts were adjusted to 2.5–3.0×10^5 platelets μL^{-1} with autologous platelet poor plasma (PPP). PRP was incubated at 37 °C to regenerate $P2X_1$ via plasma ectonucleotidases [29] for at least 30 min and recovery of $P2X_1$ was validated via platelet shape change measurements, induced by αβ-meATP [19]. When specified, mouse blood and PRP were prepared in the presence of 0.1 U mL^{-1} apyrase, to better preserve the integrity of $P2X_1$. Washed mouse platelets were prepared as described previously [17]. Platelets were resuspended in Ca^{2+}-free Tyrode's buffer (12 mM $NaHCO_3$, 0.42 mM NaH_2PO_4, 137 mM NaCl, 2.7 mM KCl, 1 mM $MgCl_2$, 5 mM HEPES, 5.5 mM glucose, 0.35% human serum albumin and 0.1 U mL^{-1} apyrase).

Light transmission during collagen induced platelet aggregation in murine PRP was recorded with a Chrono-Log Aggregometer. At least three independent experiments were performed on PRP from different pools.

Preparation and labeling of washed mouse platelets

Washed mouse platelets were resuspended in Ca^{2+}-free Tyrode's buffer, in the presence of 10 μg mL^{-1} calcein (Molecular Probes, Leiden, The Netherlands) and were incubated at 37 °C for 15 min. Labeled platelets (0.5×10^6 platelets μL^{-1} in 200 μL) from one mouse were injected into the circulation of another mouse via the catheterized jugular vein.

Shear stress induced platelet aggregation and perfusion studies

Aggregation of washed human platelets in shear stress conditions (shear induced platelet aggregation, SIPA) was carried out in a laminar shear generator, as previously described [21]. The U0126 used during SIPA was dissolved in dimethyl sulfoxide (DMSO) at 10 mM and then diluted 100-fold in saline, and further in Tyrode's buffer, containing 0.35% human serum albumin (and apyrase, when specified), to a final concentration of 1 μM. At this dilution, DMSO (0.01%) was found not to affect SIPA (not shown). Perfusion studies of calcein labeled mouse platelets over glass surfaces coated with recombinant VWF-A1 (see below) were carried out in reconstituted blood, as previously reported [30]. Perfusion studies over activated mesenteric endothelium of WT mice via online videomicroscopy was carried out as recently described [31].

Immunoblotting

Platelets (0.3 mL of platelet suspensions) were lysed in sodium dodecyl sulfate (SDS) sample buffer (62.5 mM Tris-HCl, pH 6.8, 2% SDS, 10% glycerol, 50 mM DTT, 0.1% bromophenol blue). Sample aliquots were loaded on SDS-polyacrylamide gel electrophoresis (12.5%) and subjected to Western blotting.

ERK2 and phospho-ERK2 were detected, using the Phospho-Plus p44/42 MAP Kinase Antibody kit (New England Biolabs UK Ltd, Hitchin, UK) according to the instructions of the manufacturer. Densitometric band scanning was performed, using Image J (NIH, Bethesda, MD, USA).

Photochemically induced thrombosis (PIT)

All animal experiments were reviewed and approved by the Institutional Review Board of the University of Leuven and were performed in compliance with the guidelines of the International Society on Thrombosis and Haemostasis [32]. FVB WT and TG mice (8 to 12 weeks old) were anesthetized with pentobarbital (25–35 mg kg^{-1} intraperitoneally) and the jugular vein was catheterized with a 2.5 Fr canule. Mice were positioned on a translucent table of an inverted epifluorescence microscope (Diaphot; Nikon, Melville, NY, USA) and the intestines were exposed such that the arterioles and venules covering the cecum were visualized through a Cohu CCD video camera (COHU Inc, San Diego, CA, USA). Via the jugular vein catheter, a bolus of rose bengal was injected (20 mg kg^{-1}), followed by injection of fluorescently labeled murine platelets (0.5×10^6 platelets μL^{-1} in 200 μL) and perfusion of rose bengal (20 mg kg^{-1} h^{-1}) during 30 min, the time required for the injected platelets to reach steady-state. Selected arterioles/venules were exposed for 40 s to green light, focused through the microscope objective (40 × magnification), resulting in localized and reproducible vessel wall injury over a distance of about 500 μm. Recruitment of fluorescently labeled platelets to the lesion site (adhesion and aggregation) was observed in real-time, digitized with a Scion LG3 frame grabber (Scion Corp, Frederick, ML, USA) and recorded in the memory of an attached computer for later analysis with the *NIH Image* program version 6.1. The vessel occlusion time was defined as the moment of blood flow arrest due to an occlusive thrombus in the injured arteriole or venule, that is, with flow zero.

To study the consequences on thrombus development of various inhibitors of platelet function, a bolus plus perfusion of the inhibitors tested was applied through the catheterized jugular vein 5 min prior to vessel wall injury. The following inhibitors and doses were used: the selective $P2X_1$ agonist α,β-meATP (bolus 0.16 μmol kg^{-1} = 80.8 μg kg^{-1} + infusion at 80.8 μg kg^{-1} h^{-1}), the selective $P2X_1$ receptor antagonists NF279 (bolus 0.1 μmol kg^{-1} = 150 μg kg^{-1} + infusion 150 μg kg^{-1} h^{-1}) and NF449 (bolus 0.1 μmol kg^{-1} = 168.5 μg kg^{-1} + infusion at 168.5 μg kg^{-1} h^{-1}), the MEK1/2 inhibitor U0126 (bolus 0.53 μmol kg^{-1} = 200 μg kg^{-1} + infusion at 200 μg kg^{-1} h^{-1}) and the murine GPIb antagonist VWF-A1 (bolus 0.04 μmol kg^{-1} = 2000 μg kg^{-1} + infusion at 2000 μg kg^{-1} h^{-1}). When indicated, combined inhibitor treatments were performed. In addition, inhibition of the $P2Y_{12}$ antagonist with clopidogrel (Sanofi, Toulouse, France), applied intragastrically at a dose of 20 mg kg^{-1} 24 h before analyses, was performed to evaluate the impact of interference with P2 receptors via ADP-mediated platelet activation on our thrombosis model.

Expression and purification of glutathion-S-transferase-mouse VWF-A1 fusion protein

The glutathion-S-transferase-mouse VWF A1 domain fusion protein were produced via RT-PCR from mouse platelet RNA extracts, using the following primers: forward: GTT GGA TCC ACC CCC GAG CCC CCC CTG CAC, introducing a 5′ *Bam*HI site; reverse: AT GGT CGA CCG TTT TGG TCC CGG TGA CGA, introducing a 3′ *Sal*I site. PCRs were carried out in a PTC-100 Programmable Thermal Controller (MJ Research, Inc. Watertown, MA, USA) as described before for the production of glutathion-S-transferase-human VWF-A1 domain fusion proteins [30]. The PCR product was then digested by *Bam*HI and *Sal*I, and inserted into the pGEX4T-2 vector containing the DNA sequence for GST (Amersham Pharmacia Biotech, Roosendaal, The Netherlands), and cloned [30]. Hence, a 693 bp fragment was inserted, spanning the murine A1 domain between amino acid residue Thr499 and Arg729, in traditional human residue number counting. The fusion protein expression was induced with 500 μM isopropyl-B-D-thiogalactopyranoside (IPTG) in *Escherichia coli* bacteria and the recombinant protein (VWF-A1) was purified on GST-beads, as described [30].

Statistical analysis

Comparisons between vessel occlusion times were made via two-sample test comparison, using Mann–Whitney statistical tests, described by 2-tailed P values. $P < 0.05$ was considered to be statistically significant.

Results

ERK2 activation in SIPA is not coupled to $P2X_1$

We showed earlier that SIPA strongly depends on GPIb-VWF interactions, as well as on amplification reactions by platelet released nucleotides [21]. Fig. 1A shows that the $P2X_1$ agonist L-β,γ-meATP, added just prior to initiation of SIPA, rapidly accelerated platelet aggregation at high shear rates (9000 s^{-1}). However, L-β,γ-meATP also potentiated the weak platelet aggregation observed at low shear rates (1000 s^{-1}). Figure 1B shows that at 9000 s^{-1}, SIPA was accompanied by rapid ERK2 phosphorylation in platelets, maximal at 60 s. The ERK2 phosphorylation was reversible and had completely disappeared at 3 min. Integrated density analysis (Fig. 1B) of phospho-ERK2 at 60 s revealed that the mean degree of ERK2 phosphorylation was unaffected by pre-incubation with L-β,γ-meATP, despite persistent elevation of the degree of SIPA, up to 3 min during pretreatment with L-β,γ-meATP (Fig. 1A).

Recently, we demonstrated that shear stress controlled adhesion of platelets to collagen, involves activation of ERK2 in a VWF dependent manner [22]. We therefore investigated, whether, during SIPA, $P2X_1$ was functionally coupled to ERK2 activation. Figure 1C shows, indeed, that inhibition of ERK2 activation with the MAPK kinase inhibitor

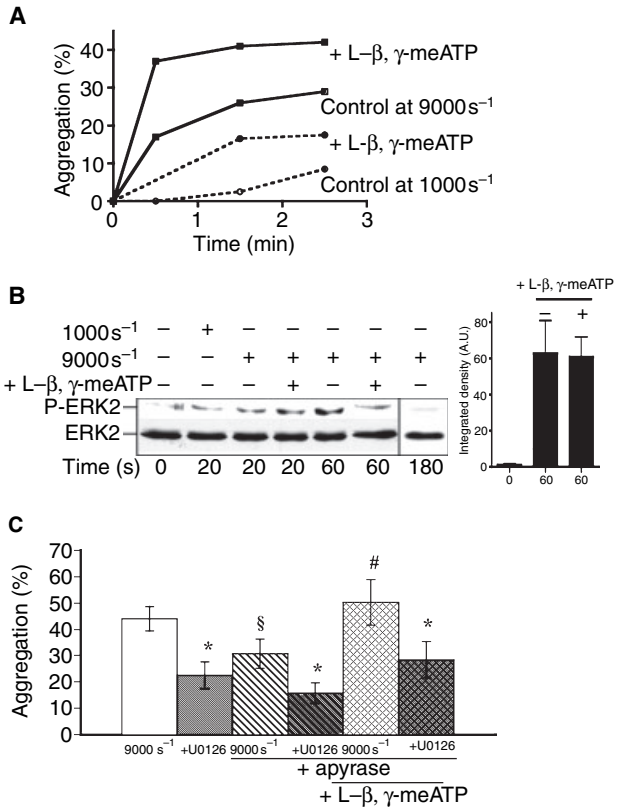

Fig. 1. ERK2 activation is SIPA is unrelated to $P2X_1$ stimulation. (A) Representative example of the degree of washed human platelet aggregation, without apyrase, at the indicated shear rate of 1000 or 9000 s^{-1}, as a function of time, in the absence or presence of L-β,γ-meATP (10 μM), added immediately prior to SIPA. (B) Western blot of total ERK2 (lower bands) and P-ERK2 (upper bands) during SIPA for the indicated time points, at 1000 or 9000 s^{-1} and with or without specific $P2X_1$ stimulation with L-β,γ-meATP (10 μM), added immediately prior to SIPA; integrated mean (±SD) band intensities for P-ERK2, at 60 s ($n = 3$), in the absence or presence of L-β,γ-meATP and compared with the averaged resting platelet P-ERK2 intensity (0 s, AU: arbitrary units). (C) Degree of washed human platelet aggregation induced at 9000 s^{-1} for 3 min, in the absence or presence of U0126 (1 μM) as indicated; the presence of apyrase (0.5 U mL^{-1}) in the platelet suspension is represented by the long horizontal line; specific $P2X_1$ stimulation with L-β,γ-meATP (10 μM), added immediately prior to SIPA is indicated via the short horizontal line (*$P < 0.005$ vs. corresponding control without inhibitor, §$P < 0.005$ vs. 9000 s^{-1}, $P = 0.001$ vs. 9000 s^{-1} + apyrase). Experiment number ranges from three (U0126 inhibition) to nine (respective controls).

U0126 reduces SIPA to 50%. In the presence of 0.5 U mL^{-1} apyrase, i.e. at a concentration that degrades ATP and ADP partially, to a degree that eliminates contributions to SIPA of ATP-$P2X_1$ and ADP-$P2Y_1$ interactions, without abolishing ADP-$P2Y_{12}$ interactions [21], U0126 still caused 50% inhibition of SIPA (Fig. 1C). Even when $P2X_1$ was stimulated with the apyrase resistant L-β,γ-meATP, just prior to SIPA, such treatment enhanced SIPA but did not affect the degree of SIPA inhibition by U0126 (Fig. 1C). These results illustrated, although ERK2 activation could be influenced by $P2X_1$ activation, that its role in SIPA was not coupled to $P2X_1$, although being coupled to GPIb-VWF (Fig. 1B) [21,22]. This finding contrasted with the $P2X_1$–ERK2 coupling during collagen-induced platelet activation in the absence of shear stress [17,19] and advocated further investigations of ERK2 in shear controlled platelet activation *in vivo*.

Inhibition of platelet aggregation by $P2X_1$ antagonists

Prior to *in vivo* studies, NF449 and NF279, both suramin analogs, exhibiting high potency in inhibiting $P2X_1$ in other systems and highly selective over other P2X ion channels and P2Y receptor inhibitors [26,33], were tested in platelet aggregation. Low concentrations of NF279 substantially inhibited the collagen-induced aggregation of human (not shown) and of murine WT platelets (Fig. 2A), at least when aggregation was induced at collagen concentrations below 0.5 μg mL^{-1}, in agreement with the known function of $P2X_1$ in low-dose collagen-induced platelet aggregation [28]. When $P2X_1$ was desensitized via pretreatment of platelets with α,β-meATP, the subsequent collagen-induced aggregation was no longer affected by NF279 (data not shown), confirming the specificity of $P2X_1$ inhibition by NF279 during aggregation. When tested in the presence of low concentrations of apyrase, to more optimally preserve $P2X_1$ function, NF449 potently inhibited

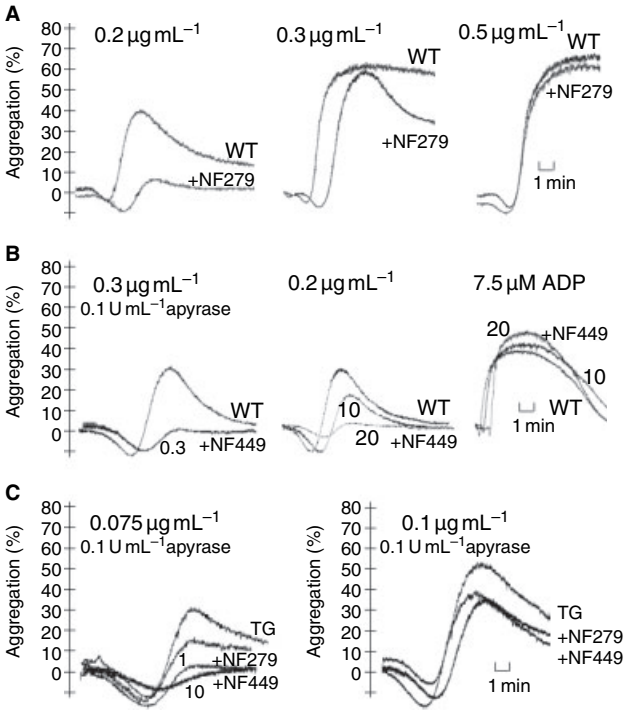

Fig. 2. $P2X_1$ antagonism during collagen-induced aggregation. (A) Aggregation tracings of WT mouse hirudinized, apyrase-free platelet-rich plasma by the indicated concentration of collagen, in the presence or absence of NF279 (1 μM). (B) Aggregation of WT mouse hirudinized, platelet-rich plasma by collagen (0.2 or 0.3 μg mL^{-1}, as indicated) or ADP, in the presence or absence of 0.1 U mL^{-1} apyrase and NF449 (0.3, 10 or 20 μM), as indicated. (C) Aggregation of TG mouse hirudinized, platelet-rich plasma by collagen, in the presence of 0.1 U mL^{-1} apyrase and NF279 (1 μM) or NF449 (1 or 10 μM, as indicated, or 1 μM in the right panel).

the low dose collagen-induced platelet aggregation of WT platelets, as recently reported [33] and as potently as NF279 (Fig. 2B). When tested in apyrase-free platelet-rich plasma, higher concentrations of NF449 were required to inhibit the collagen-induced platelet aggregation. Nevertheless, aggregation of WT mouse PRP by 5 or 7.5 μM ADP was not inhibited at these concentrations of NF449 (Fig. 2B). Likewise, NF279 and NF449 inhibited the weak aggregation of murine TG platelets, overexpressing human P2X1, but not the stronger aggregation, induced by slightly higher collagen concentrations (Fig. 1C). These findings illustrate that NF279 and NF449 reduced platelet aggregation by collagen in PRP, in a manner formally similar to $P2X_1$ desensitization with α,β-meATP [28], enabling their use for the *in vivo* study of thrombosis, i.e. when tested at low plasma concentrations, thus avoiding interference of the ADP mediated activation of $P2Y_1$ [33].

Arteriolar and venular thrombosis in WT and TG mice

To study the role of platelet $P2X_1$ and ERK2 in shear stress-controlled thrombosis *in vivo*, we used a model of photochemical blood vessel injury in WT and TG mice, focusing both on arteriolar and venular thrombosis. Thrombus formation was constantly monitored microscopically in real time until vessel occlusion. Figure 3A shows a series of chronological images of developing thrombosis in the arteriolar and venular circulation of WT and TG mice. To characterize contributions to thrombosis of $P2X_1$ vs. the central role of $P2Y_{12}$ in platelet activation amplification [15], mice were also treated with clopidogrel. This treatment strongly delayed arteriolar vessel occlusion (WT: 38 ± 8 min, $n = 13$; WT + clopidogrel: 102 ± 1 min, $n = 3$; values: mean ± SD, $P < 0.01$) (not shown), confirming that $P2Y_{12}$, activated by released ADP, is instrumental in this thrombosis model. TG mice showed nearly immediate arteriolar vessel occlusion following photochemical injury (Fig. 3A), corroborating our previous findings [17] that $P2X_1$ overexpression promotes thrombosis. Nevertheless, treatment of TG mice with clopidogrel strongly inhibited thrombus formation (arteriolar vessel occlusion time = 99 ± 7.8 min, $n = 3$, $P = 0.015$, not shown), which therefore still largely depended in TG mice on $P2Y_{12}$.

To neutralize VWF in the mouse, a recombinant mouse VWF A1 domain (VWF-A1) was produced and validated *in vitro* and *in vivo*. During perfusion studies of calcein-labeled platelets over glass surface coated VWF-A1, platelet rolling was supported at a shear rate of 600 s^{-1}, but not 300 s^{-1} (not shown); this interaction was inhibited by soluble VWF-A1, added to the perfusate, as a consequence of competition with surface coated VWF-A1 for binding to platelet GPIb (Fig. 3B). Further *in vivo* validation during the recording of platelet tethering over A23187 activated endothelium of mouse mesenteric blood vessels, confirmed that, in mice, VWF-A1 was capable of reducing the VWF mediated rolling of circulating platelets over A23187 activated endothelial cells (Fig. 3C). This fragment was therefore selected to pharmacologically inhibit VWF during our thrombosis studies.

Importance of $P2X_1$ activity in arteriolar and venular thrombosis

In vivo desensitization of $P2X_1$ in WT mice by an i.v. bolus of α,β-meATP, followed by a continuous infusion, aiming to achieve an initial plasma concentration of 2 μM, prior to injury induction delayed arteriolar vessel occlusion from 38 ± 8 min to 74 ± 2 min. An i.v. bolus of NF279, followed by an infusion, aiming to achieve an initial plasma concentration of 1.25 μM, likewise, delayed arteriolar vessel occlusion to 75 ± 10 min. An i.v. bolus of NF449, followed by an infusion, aiming to equally achieve an initial plasma concentration of 1.25 μM, delayed arteriolar vessel occlusion to 79 ± 6 min (Fig. 4A). The identical treatments of TG mice with α,β-meATP delayed occlusion from 4.3 ± 2.3 min to 68 ± 3.1 min, with NF279 to 60 ± 6.7 min and with NF449 to 68 ± 2.6 min. Taken together, these data demonstrate that platelet $P2X_1$ is involved in the regulation of arterial thrombosis and underscore that the pharmacological inhibition of $P2X_1$ by low plasma concentrations of NF279 or NF449 is equipotent in WT and TG mice. Furthermore, $P2X_1$ inhibition and inactivation via desensitization with its agonist α,β-meATP reduce the role of $P2X_1$ in thrombosis to the same degree.

Whereas overexpression of $P2X_1$ in TG mice strongly shortened arteriolar occlusion times, it affected venular occlusion times more weakly (19 ± 12 min), compared with the WT control values (48 ± 4.5 min; Fig. 4B). Correspondingly, α,β-meATP, NF279 and NF449 only moderately affected venular occlusion times in WT mice to 66 ± 10, 56 ± 10 and 70 ± 5.3 min respectively. In TG mice, as expected, more pronounced inhibition was noted, however to comparable occlusion times, averaging 69 ± 7, 52 ± 15 and 64 + 2.2 min in α,β-meATP, NF279 and NF449 treated mice, respectively. These findings illustrate that shear stress is a crucial component of $P2X_1$ regulation *in vivo*.

Pooled analysis in venular thrombosis for WT and TG mice revealed a mean occlusion time (67 ± 8.4 min, $n = 10$) during desensitization with α,β-meATP, identical to the mean occlusion time (67 ± 5 min, $n = 8$), achieved during antagonism with NF449. These values are significantly longer than the mean occlusion time (54 ± 12 min, $n = 8$) during treatment with NF279 ($P < 0.05$). Therefore, low concentrations of NF449 appeared more potent than NF279, motivating its further selection as an inhibitor to neutralize $P2X_1$ function.

ERK2 phosphorylation is involved in arteriolar thrombosis

Platelet aggregation by VWF (induced via ristocetin) involves ERK2 activation and VWF binding to GPIbα causes phosphorylation of ERK2 [34]. Because we found shear stress dependent ERK2 phosphorylation to be coupled to VWF binding to GPIbα during platelet-collagen interactions [22], but not to $P2X_1$ (Fig. 1), the role of the ERK2 pathway in arteriolar vs. venular thrombosis was investigated, via administration of that dose of U0126, known to prevent

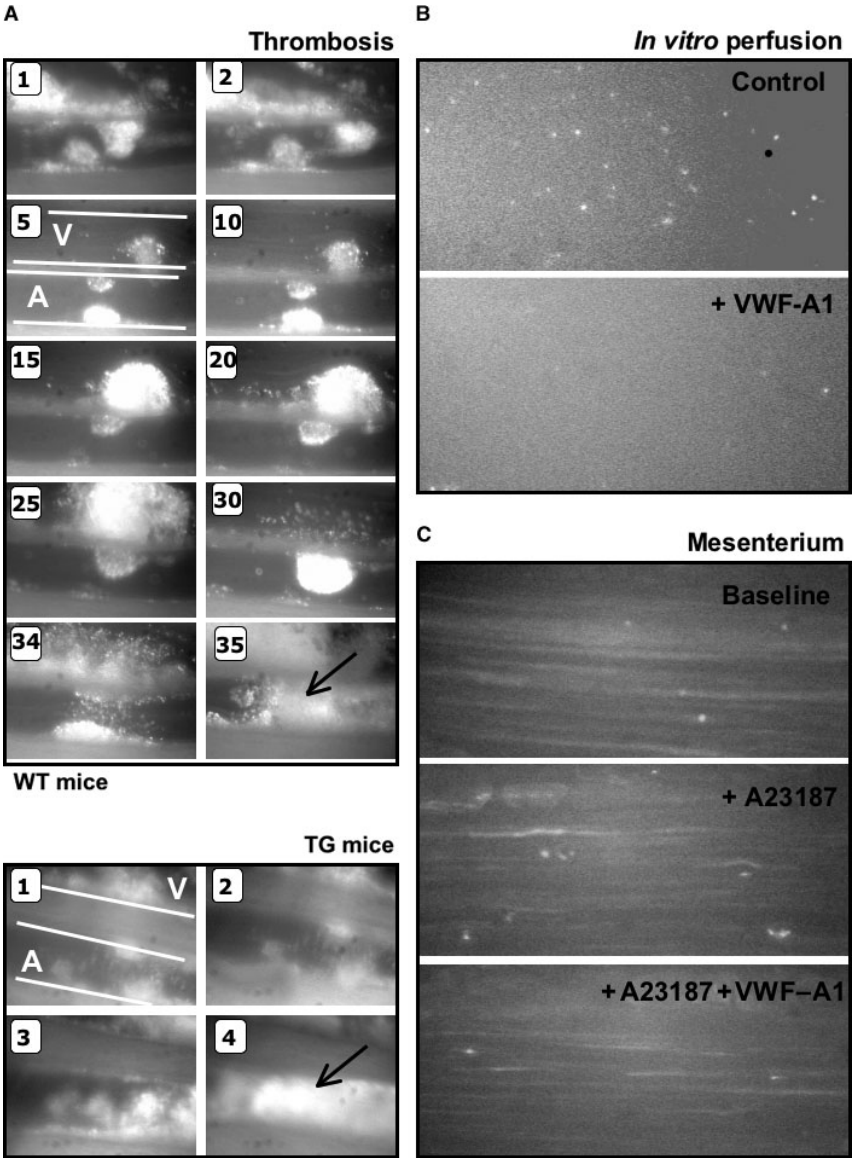

Fig. 3. Dynamics of intestinal thrombosis and VWF neutralization. (A) Representative photographs and time course (indicated in minutes in inserts) of thrombus formation induced by photochemical injury of WT (upper series) and TG (lower series) mouse intestinal arterioles (A) and venules (V). Selected arterioles and venules irrigating the cecum had a diameter of 60–100 μm. Arrows depict irreversible arteriolar vessel occlusion; the early reversible thrombotic responses (1–2 min) were not analyzed. (B) *In vitro* perfusion of calcein-labeled WT mouse platelets, perfused over VWF-A1 coated glass surfaces (control) and inhibition of tethering by VWF-A1 (50 μg mL^{-1}) added to the perfusate (+VWF-A1). (C) Tethering of injected calcein-labeled WT mouse platelets in mesenteric blood vessels, before endothelial cell activation (baseline) and following activation with A23187 (30 μM), in the absence (+A23187) or presence of VWF-A1 (+A23187 + VWF-A1; bolus 0.04 μmol kg^{-1} + infusion 0.04 μmol kg^{-1} h^{-1}); pictures show individual platelets, tethering on the vessel wall endothelium.

mortality in an experimental model of pulmonary thromboembolism, partially in WT mice and completely in TG mice [17]. Figure 5 shows how the mean arteriolar vessel occlusion time is moderately, but significantly prolonged in WT mice by U0126 to 51 ± 17 min. Nevertheless, the vessel occlusion time distribution ranged from 19 to 64 min ($n = 11$), compared with a vessel occlusion time distribution, ranging from 21 to 48 min in non-treated controls ($n = 13$). This finding suggested a moderate and variable role for ERK2 during platelet activation, involved in most, but not all animals. However, the narrower arteriolar occlusion time distribution in TG mice, as well as the significant arteriolar vessel occlusion prolongation by U0126 to 41 ± 10 min provided evidence for a role for ERK2 activation in thrombosis in TG mice. Venular occlusion times, on the contrary, were weakly affected by U0126 treatment in WT (56 ± 6.1 min) mice, but appeared still prolonged in TG mice (46 ± 5.3 min). These findings uncovered a more important role for ERK2 in arteriolar than in venular thrombosis, but did not allow distinction between VWF

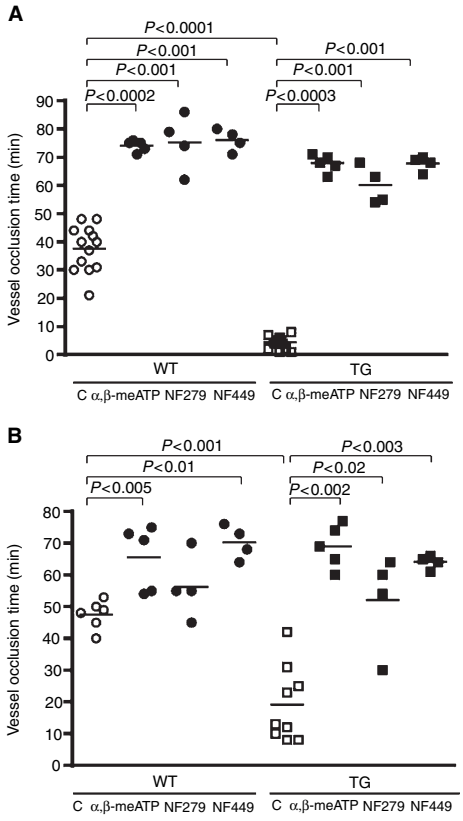

Fig. 4. Inactivation of $P2X_1$ in intestinal blood vessel thrombosis. Representative dot plots of occlusion times in arterioles (A) and venules (B) during photochemically induced thrombosis in WT and TG mice; WT and TG mice were treated with the $P2X_1$ agonist αβ-meATP (bolus 0.16 μmol kg^{-1} + infusion 0.16 μmol kg^{-1} h^{-1}) and with the $P2X_1$ antagonists NF279 (bolus 0.1 μmol kg^{-1} + infusion 0.1 μmol kg^{-1} h^{-1}) and NF449 (bolus 0.1 μmol kg^{-1} + infusion 0.1 μg-mole kg^{-1} h^{-1}) as indicated; two-tailed *P* values were calculated via two-column Mann–Whitney comparison.

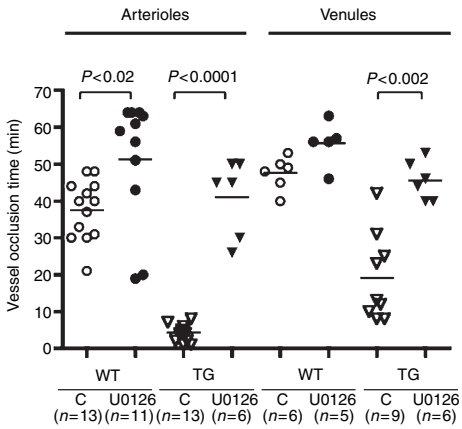

Fig. 5. Role of ERK2 in intestinal blood vessel thrombosis. Representative dot plots of occlusion times in arterioles and venules, as indicated, during photochemically induced thrombosis in WT and TG mice, treated with U0126 (bolus 0.53 μmol kg^{-1} + infusion 0.53 μmol kg^{-1} h^{-1}) for the number of mice indicated. Control values are the same as in Fig. 4; two-tailed *P* values were calculated via two-column Mann–Whitney comparison.

dependent vs. $P2X_1$ mediated ERK2 activation in the TG mice. Nevertheless, no significant differences were found between occlusion times in U0126 treated WT and TG mice, neither for arteriolar, nor for venular comparisons.

ERK2 activation in arteriolar thrombosis is coupled to GPIb activation

To further investigate the respective role of GPIb and $P2X_1$ in ERK2 activation during thrombosis, its phosphorylation was blocked by U0126 in the context of GPIb inhibition and $P2X_1$ inhibition respectively, both in WT (Fig. 6) and TG mice (Fig. 7). The most striking finding of this analysis was that VWF inactivation by VWF-A1 resulted in very similar arteriolar occlusion times in WT (58 ± 7.4 min) and TG (56 ± 4.2 min) mice. Likewise, venular occlusion times were similarly prolonged in WT (55 ± 7 min) and TG (57 ± 4.6 min) mice, during treatment with VWF-A1 (Figs 6 and 7). The combined treatment with U0126 + VWF-A1 only mildly further prolonged arteriolar occlusion times in WT (68 ± 2.9 min) and TG (68 ± 2.2 min) mice, to identical values, compared with VWF-A1 treated mice (Figs 6 and 7). Likewise, combined treatment with U0126 + NF449 mildly prolonged arteriolar occlusion times in WT (84 ± 4.6 min) and TG (78 ± 3.3 min) mice, compared with NF449 treated mice (Figs 6 and 7).

The combined treatment with U0126 + VWF-A1 prolonged venular occlusion times in WT (74 ± 6.7 min) and TG (60 ± 4.8 min) mice, compared with VWF-A1 treated mice (Figs 6 and 7). Finally, the combined treatment with U0126 + NF449 clearly prolonged venular occlusion times in WT (84 ± 6.2 min) and TG (86 ± 3.2 min), compared with NF449 treated mice (Figs 6 and 7).

Discussion

Murine thrombosis depends on VWF-GPIbα and VWF-$\alpha_{IIb}\beta_3$ interactions [35], fibrinogen-$\alpha_{IIb}\beta_3$ interactions [35] as well as on fibronectin-$\alpha_5\beta_1$ interactions [36]. Secondary amplification pathways, involving $P2Y_1$ [11,16], $P2Y_{12}$ [14,15] and $P2X_1$ [18,33] are essential in controlling thrombus growth [13]. Also in the presently applied thrombosis model, clopidogrel behaves as a potent antithrombotic: a single dose strongly prevented vessel wall injury-triggered thrombus formation in arterioles and venules of the murine intestinal circulation. We therefore used this platelet-dependent model to evaluate the role of ERK2 in thrombosis, in relation to pathways studied before, such as activation of the GPIb-VWF pathway [21,22] and $P2X_1$ mediated ERK2 activation occurring during the collagen-induced platelet aggregation [19,20]. Using TG mice overexpressing platelet human $P2X_1$, we confirm a role for $P2X_1$, which is more pronounced but not limited to high shear stress conditions. Hence, in TG mice, arteriolar thrombosis was more strongly intensified than venular thrombosis, compared with WT mice. Correspondingly, pharmacological inhibition of thrombosis by the $P2X_1$ antagonists NF279 and NF449 was

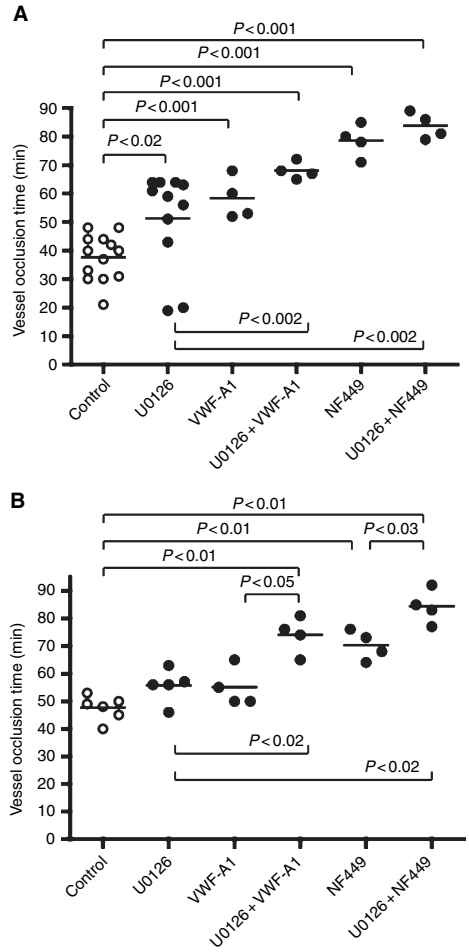

Fig. 6. Double inhibition strategy in WT mouse thrombosis. Representative dot plots of occlusion times in arterioles (A) and venules (B), during photochemically induced thrombosis. Occlusion times are for mice treated with U0126 (bolus 0.53 μmol kg^{-1} + infusion 0.53 μmol kg^{-1} h^{-1}), with VWF-A1 (bolus 0.04 μmol kg^{-1} + infusion 0.04 μmol kg^{-1} h^{-1}), alone or combined with U0126 and with NF 449 (bolus 0.1 μmol kg^{-1} + infusion 0.1 μmol kg^{-1} h^{-1}), alone or combined with U0126; Control and U0126, respectively NF449 values are the same as in Figs 4 and 5; two-tailed *P* values were calculated via two-column Mann–Whitney comparison.

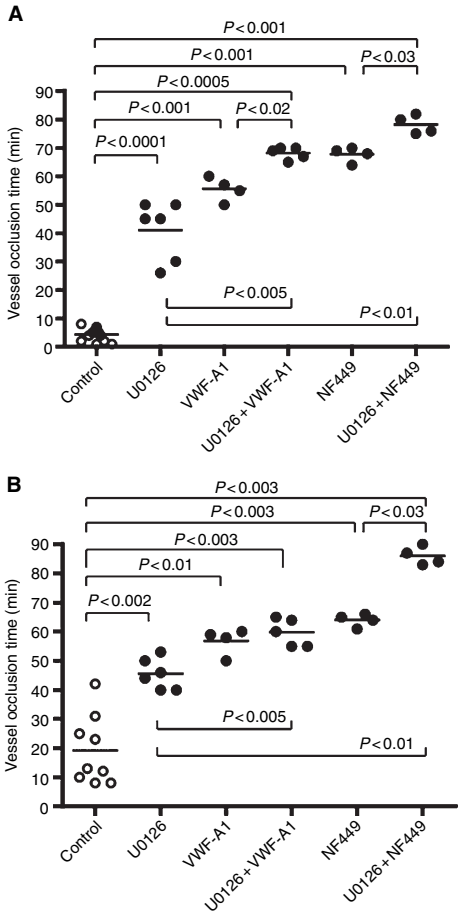

Fig. 7. Double inhibition strategy in TG mouse thrombosis. Representative dot plots of occlusion times in arterioles (A) and venules (B), during photochemically induced thrombosis. Occlusion times are for mice treated with U0126 (bolus 0.53 μmol kg^{-1} + infusion 0.53 μmol kg^{-1} h^{-1}), with VWF-A1 (bolus 0.04 μmol kg^{-1} + infusion 0.04 μmol kg^{-1} h^{-1}), alone or combined with U0126 and with NF 449 (bolus 0.1 μmol kg^{-1} + infusion 0.1 μmol kg^{-1} h^{-1}), alone or combined with U0126; Control and U0126, respectively NF449 values are the same as in Figs 4 and 5; two-tailed *P* values were calculated via two-column Mann–Whitney comparison.

more pronounced in arteriolar than in venular thrombosis, but was operative in both. Desensitization of $P2X_1$ with α,β-meATP yielded similar inhibition of thrombosis as $P2X_1$ antagonism, adding to the specificity of NF449, at least when used at low concentrations. Moreover, the degree of inhibition of thrombosis in WT and TG mice by NF449 was comparable, compatible with saturated $P2X_1$ occupation at the dose regimen applied, also in TG mice.

Although not activated by ADP and its potent analogue 2-methylthio-ADP, platelet stimulation with thrombin induces ERK2 activation in a manner, highly dependent on ADP secretion and $P2Y_{12}$ receptor signaling [25]. These findings were explained via primary signaling through Gq and subsequent coupling via Gi by the $P2Y_{12}$ receptor. Other reports have also demonstrated that a coordinated pathway through both Gq from TxA_2 and Gi from ADP was necessary for ERK2 activation *in vitro* [37]. In view of the importance of ERK2 activation in controlling platelet aggregation by collagen [20], as well as in SIPA (this study), we presently studied further the importance of ERK2 activation during *in vivo* thrombosis, in relation to shear stress controlled signaling processes. The MEK 1/2 inhibitor, U0126, at a concentration blocking ERK2 activation, mildly prolonged arteriolar occlusion times in WT mice, but not all animals responded to this inhibitor. In contrast, a more homogeneous and clear prolongation of arteriolar occlusion times was found in TG mice, confirming a role *in vivo* for the ERK2 pathway. Similarly to the role of $P2X_1$ in thrombosis, ERK2 was found to be more important in arteriolar thrombosis, because in TG mice, the relative effect of U0126 was smaller on venular thrombosis, but U0126 reduced thrombosis to a similar degree in WT and TG venules.

We have shown before that inhibition of SIPA by GPIb or VWF neutralization leads to a twofold reduction in the extent of platelet dense granule release [21], hence reducing amplifi-

cation waves of platelet activation by secreted ADP and ATP. In addition, nucleotide antagonism also reduces platelet degranulation by about 30% [21]. Therefore, neutralization of the GPIb-VWF axis will strongly reduce nucleotide contributions to thrombosis, also in our *in vivo* model. This interpretation explains our present findings during inhibition of GPIb-VWF interactions by the recombinant murine VWF-A1 domain. This fragment is capable of competing with murine VWF for the recruitment of platelets, a phenomenon largely dependent on VWF [38]. The finding that VWF-A1 reduces the thrombotic response in WT and TG mice to comparable occlusion times, despite extra platelet activation and shorter occlusion times in non-treated TG mice, implies that inhibition by VWF-A1 abrogates both initial adhesion of platelets, as well as subsequent amplification pathways, under control of released ATP. Hence, the interpretation that GPIb-VWF interaction inhibition slows down platelet recruitment to the vessel wall, platelet degranulation and subsequent nucleotide activation amplification, is compatible with classical concepts of thrombus formation [1,2].

These findings therefore implicate that GPIb inactivation inhibits potential GPIb-, as well as $P2X_1$ mediated contributions of ERK2 to thrombosis. In addition, the small differences in occlusion times during inhibition by VWF-A1 vs. U0126 + VWF-A1, measured in WT and TG mice, then reflect relatively minor contributions to thrombosis for GPIb-VWF independent ERK2 signaling, such as via Src kinase [39]. Also, although our thrombosis studies did not allow a formal distinction between a role for GPIb mediated or subsequent $P2X_1$ mediated ERK2 signaling, SIPA *in vitro* identified that ERK2 was involved in shear induced platelet activation, but independently of $P2X_1$. Hence, the more pronounced relative inhibition of thrombosis by U0126 in TG than in WT mice can then be explained by a comparable prevention of VWF mediated signaling in WT and TG mice and by the more pronounced consequences of this inhibition during secondary amplification in TG, compared with WT mice. In addition, comparison of occlusion times during inhibition by U0126 vs. U0126 + VWF-A1 in WT and TG mice, confirms the existence of ERK2 independent contributions to thrombosis by platelet GPIb activation. The relatively smaller prolongation of occlusion times by VWF-A1 in WT and TG venules than in arterioles can be explained by a smaller role for VWF in venular than in arteriolar thrombosis [40] and by a smaller response of platelet $P2X_1$ in venules to an already reduced release of ATP.

We have shown before that $P2X_1$ neutralization reduced SIPA about twofold in human platelet aggregation [21]. Presently, we observed that NF449 prolongs occlusion times in WT and even in TG mice to values, even slightly longer than found during VWF-A1 inhibition, indicative of potent inhibition of secondary platelet activation, even when the initial platelet recruitment on injured vessel walls is preserved, in the presence of NF449. Occlusion times were only mildly prolonged further in U0126 + NF449 treated mice, compared with NF449 treatment alone. The interpretation that ERK2 largely operates via GPIb mediated signaling, even during the inhibition by NF449 and the U0126 + NF449 combination, is supported in this set of experiments by analysis in WT mice of the delay in occlusion during treatment with NF449, in the absence or presence of ERK2 signaling. In WT arterioles NF449 treatment delays the mean occlusion by 41 min, from 38 to 79 min; during U0126 treatment, the mean occlusion time is delayed by 33 min from 51 to 84 min in U0126 + NF449 treated animals. Likewise, in WT venules, NF449 treatment delays the mean occlusion by 22 min, from 48 to 70 min; during U0126 treatment, the mean occlusion time is delayed by 28 min from 56 to 84 min in U0126 + NF449 treated animals. This comparison reveals that $P2X_1$ in thrombosis acts independently of ERK2, inhibition of the latter having no effect on $P2X_1$ in thrombosis.

Although previously, we have coupled the activation of ERK2 and $P2X_1$ stimulation in the context of collagen-induced platelet activation, our present findings link ERK2 activation to VWF signaling. It therefore appears that in the present shear stress thrombosis model, collagen mediated ERK2 signaling, as found in static conditions [19], is not operational. Although, in the rose-bengal model studied, contributions of subendothelial collagen to thrombosis may be limited, this conclusion complies with the role of ERK2 during perfusion studies over collagen [22], where ERK2 phosphorylation can also strictly be coupled to VWF mediated platelet adhesion and activation, rather than to direct collagen–platelet interactions.

In conclusion, the present study, using wild type and TG mice with specific platelet $P2X_1$ gain-of-function, has shown that $P2X_1$ and ERK2 contribute to platelet activation and thrombosis in a shear controlled manner and that ERK2 activation is coupled to platelet GPIb mediated signal transduction predominantly.

Acknowledgements

This work was supported by the FWO Vlaanderen (project nr G.0227.03) and the University of Leuven (project GOA/2004/09). During this study, C.O. was the recipient of a postdoctoral Fellowship from the FWO Vlaanderen and was a Scientific Research Worker FNRS; K.D. received a junior Fellowship from the University Hospital Leuven.

References

1 Andrews RK, Shen Y, Gardiner EE, Berndt MC. Platelet adhesion receptors and (patho)physiological thrombus formation. *Histol Histopathol* 2001; **16**: 969–80.
2 Ruggeri ZM. Von Willebrand factor. *Curr Opin Hematol* 2003; **10**: 142–9.
3 Siljander PR, Munnix IC, Smethurst PA, Deckmyn H, Lindhout T, Ouwehand WH, Farndale RW, Heemskerk JW. Platelet receptor interplay regulates collagen-induced thrombus formation in flowing human blood. *Blood* 2004; **103**: 1333–41.
4 Nieswandt B, Watson SP. Platelet-collagen interaction: is GPVI the central receptor? *Blood* 2003; **102**: 449–61.

5 Barstad RM, Orvim U, Hamers MJ, Tjonnfjord GE, Brosstad FR, Sakariassen KS. Reduced effect of aspirin on thrombus formation at high shear and disturbed laminar blood flow. *Thromb Haemost* 1996; **75**: 827–32.

6 Rao AK. Congenital disorders of platelet function: disorders of signal transduction and secretion. *Am J Med Sci* 1998; **316**: 69–76.

7 Hoylaerts MF, Oury C, Toth-Zsamboki E, Vermylen J. ADP receptors in platelet activation and aggregation. *Platelets* 2000; **11**: 307–9.

8 Angelillo-Scherrer A, de Frutos P, Aparicio C, Melis E, Savi P, Lupu F, Arnout J, Dewerchin M, Hoylaerts M, Herbert J, Collen D, Dahlback B, Carmeliet P. Deficiency or inhibition of Gas6 causes platelet dysfunction and protects mice against thrombosis. *Nat Med* 2001; **7**: 215–21.

9 Dogne JM, Rolin S, de Leval X, Benoit P, Neven P, Delarge J, Kolh P, Damas J, David JL, Masereel B. Pharmacology of the thromboxane receptor antagonist and thromboxane synthase inhibitor BM-531. *Cardiovasc Drug Rev* 2001; **19**: 87–96.

10 Drouet L. Atherothrombosis as a systemic disease. *Cerebrovasc Dis* 2002; **13**(Suppl. 1): 1–6.

11 Gachet C. Identification, characterization, and inhibition of the platelet ADP receptors. *Int J Hematol* 2001; **74**: 375–81.

12 Rolf MG, Brearley CA, Mahaut-Smith MP. Platelet shape change evoked by selective activation of P2X1 purinoceptors with alpha,beta-methylene ATP. *Thromb Haemost* 2001; **85**: 303–8.

13 van Gestel MA, Heemskerk JW, Slaaf DW, Heijnen VV, Reneman RS, oude Egbrink MG. In vivo blockade of platelet ADP receptor P2Y12 reduces embolus and thrombus formation but not thrombus stability. *Arterioscler Thromb Vasc Biol* 2003; **23**: 518–23.

14 Savi P, Labouret C, Delesque N, Guette F, Lupker J, Herbert JM. P2y(12), a new platelet ADP receptor, target of clopidogrel. *Biochem Biophys Res Commun* 2001; **283**: 379–83.

15 Andre P, Delaney SM, LaRocca T, Vincent D, DeGuzman F, Jurek M, Koller B, Phillips DR, Conley PB. P2Y12 regulates platelet adhesion/activation, thrombus growth, and thrombus stability in injured arteries. *J Clin Invest* 2003; **112**: 398–406.

16 Lenain N, Freund M, Leon C, Cazenave JP, Gachet C. Inhibition of localized thrombosis in P2Y1-deficient mice and rodents treated with MRS2179, a P2Y1 receptor antagonist. *J Thromb Haemost* 2003; **1**: 1144–9.

17 Oury C, Kuijpers MJ, Toth-Zsamboki E, Bonnefoy A, Danloy S, Vreys I, Feijge MA, De Vos R, Vermylen J, Heemskerk JW, Hoylaerts MF. Overexpression of the platelet P2X1 ion channel in transgenic mice generates a novel prothrombotic phenotype. *Blood* 2003; **101**: 3969–76.

18 Hechler B, Lenain N, Marchese P, Vial C, Heim V, Freund M, Cazenave JP, Cattaneo M, Ruggeri ZM, Evans R, Gachet C. A role of the fast ATP-gated P2X1 cation channel in thrombosis of small arteries in vivo. *J Exp Med* 2003; **198**: 661–7.

19 Oury C, Toth-Zsamboki E, Vermylen J, Hoylaerts MF. P2X(1)-mediated activation of extracellular signal-regulated kinase 2 contributes to platelet secretion and aggregation induced by collagen. *Blood* 2002; **100**: 2499–505.

20 Toth-Zsamboki E, Oury C, Cornelissen H, De Vos R, Vermylen J, Hoylaerts MF. P2X1-mediated ERK2 activation amplifies the collagen-induced platelet secretion by enhancing myosin light chain kinase activation. *J Biol Chem* 2003; **278**: 46661–7.

21 Oury C, Sticker E, Cornelissen H, De Vos R, Vermylen J, Hoylaerts MF. ATP augments von Willebrand factor-dependent shear-induced platelet aggregation through Ca2+–calmodulin and myosin light chain kinase activation. *J Biol Chem* 2004; **279**: 26266–73.

22 Mazharian A, Roger S, Maurice P, Berrou E, Popoff MR, Hoylaerts MF, Fauvel-Lafeve F, Bonnefoy A, Bryckaert M. Differential involvement of ERK2 and p38 in platelet adhesion to collagen. *J Biol Chem* 2005; **280**: 26002–10.

23 Bugaud F, Nadal-Wollbold F, Levy-Toledano S, Rosa JP, Bryckaert M. Regulation of c-jun-NH2 terminal kinase and extracellular-signal regulated kinase in human platelets. *Blood* 1999; **94**: 3800–5.

24 Nadal-Wollbold F, Pawlowski M, Levy-Toledano S, Berrou E, Rosa JP, Bryckaert M. Platelet ERK2 activation by thrombin is dependent on calcium and conventional protein kinases C but not Raf-1 or B-Raf. *FEBS Lett* 2002; **531**: 475–82.

25 Falker K, Lange D, Presek P. ADP secretion and subsequent P2Y12 receptor signalling play a crucial role in thrombin-induced ERK2 activation in human platelets. *Thromb Haemost* 2004; **92**: 114–23.

26 Rettinger J, Schmalzing G, Damer S, Muller G, Nickel P, Lambrecht G. The suramin analogue NF279 is a novel and potent antagonist selective for the P2X(1) receptor. *Neuropharmacology* 2000; **39**: 2044–53.

27 Jacobson KA, Mamedova L, Joshi BV, Besada P, Costanzi S. Molecular recognition at adenine nucleotide (p2) receptors in platelets. *Semin Thromb Hemost* 2005; **31**: 205–16.

28 Oury C, Toth-Zsamboki E, Thys C, Tytgat J, Vermylen J, Hoylaerts MF. The ATP-gated P2X1 ion channel acts as a positive regulator of platelet responses to collagen. *Thromb Haemost* 2001; **86**: 1264–71.

29 Glenn JR, White AE, Johnson A, Fox SC, Behan MW, Dolan G, Heptinstall S. Leukocyte count and leukocyte ecto-nucleotidase are major determinants of the effects of adenosine triphosphate and adenosine diphosphate on platelet aggregation in human blood. *Platelets* 2005; **16**: 159–70.

30 Bonnefoy A, Yamamoto H, Thys C, Kito M, Vermylen J, Hoylaerts MF. Shielding the front-strand beta 3 of the von Willebrand factor A1 domain inhibits its binding to platelet glycoprotein Ibalpha. *Blood* 2003; **101**: 1375–83.

31 Appeldoorn CC, Bonnefoy A, Lutters BC, Daenens K, van Berkel TJ, Hoylaerts MF, Biessen EA. Gallic acid antagonizes P-selectin-mediated platelet-leukocyte interactions: implications for the French paradox. *Circulation* 2005; **111**: 106–12.

32 Giles AR. Guidelines for the use of animals in biomedical research. *Thromb Haemost* 1987; **58**: 1078–84.

33 Hechler B, Magnenat S, Zighetti ML, Kassack MU, Ullmann H, Cazenave JP, Evans R, Cattaneo M, Gachet C. Inhibition of platelet functions and thrombosis through selective or non selective inhibition of the platelet P2 receptors with increasing doses of Nf449. *J Pharmacol Exp Ther* 2005; **314**: 232–43.

34 Li Z, Xi X, Du X. A mitogen-activated protein kinase-dependent signaling pathway in the activation of platelet integrin alpha IIbbeta3. *J Biol Chem* 2001; **276**: 42226–32.

35 Ni H, Denis CV, Subbarao S, Degen JL, Sato TN, Hynes RO, Wagner DD. Persistence of platelet thrombus formation in arterioles of mice lacking both von Willebrand factor and fibrinogen. *J Clin Invest* 2000; **106**: 385–92.

36 Ni H, Yuen PS, Papalia JM, Trevithick JE, Sakai T, Fassler R, Hynes RO, Wagner DD. Plasma fibronectin promotes thrombus growth and stability in injured arterioles. *Proc Natl Acad Sci USA* 2003; **100**: 2415–9.

37 Roger S, Pawlowski M, Habib A, Jandrot-Perrus M, Rosa JP, Bryckaert M. Costimulation of the Gi-coupled ADP receptor and the Gq-coupled TXA2 receptor is required for ERK2 activation in collagen-induced platelet aggregation. *FEBS Lett* 2004; **556**: 227–35.

38 Theilmeier G, Michiels C, Spaepen E, Vreys I, Collen D, Vermylen J, Hoylaerts MF. Endothelial von Willebrand factor recruits platelets to atherosclerosis-prone sites in response to hypercholesterolemia. *Blood* 2002; **99**: 4486–93.

39 Marshall SJ, Senis YA, Auger JM, Feil R, Hofmann F, Salmon G, Peterson JT, Burslem F, Watson SP. GPIb-dependent platelet activation is dependent on Src kinases but not MAP kinase or cGMP-dependent kinase. *Blood* 2004; **103**: 2601–9.

40 Yamamoto H, Vreys I, Stassen JM, Yoshimoto R, Vermylen J, Hoylaerts MF. Antagonism of vWF inhibits both injury induced arterial and venous thrombosis in the hamster. *Thromb Haemost* 1998; **79**: 202–10.